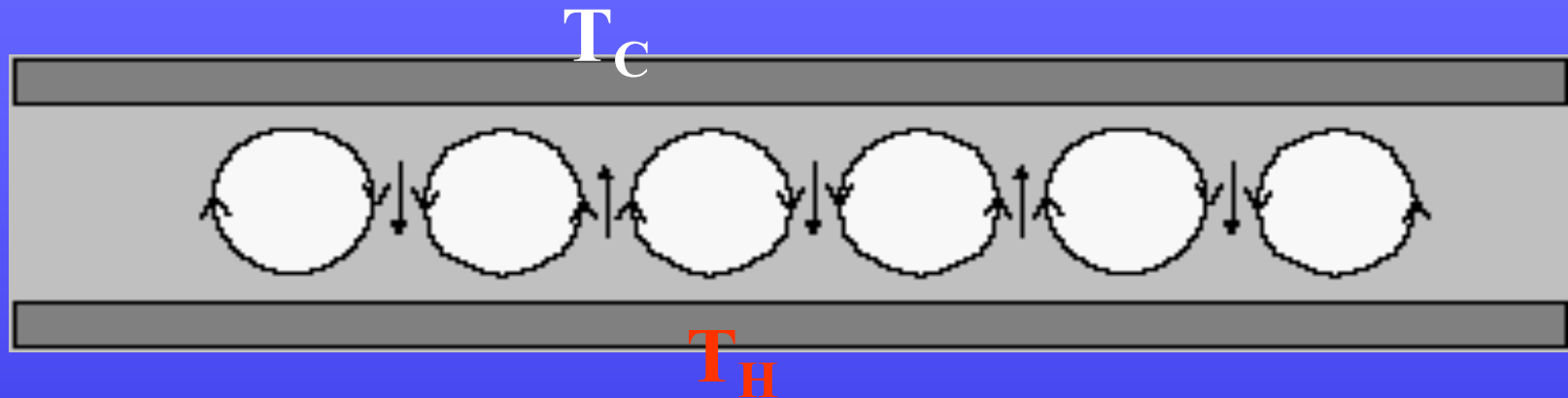


CONTROL OF Rayleigh-Bénard (RB) CONVECTION

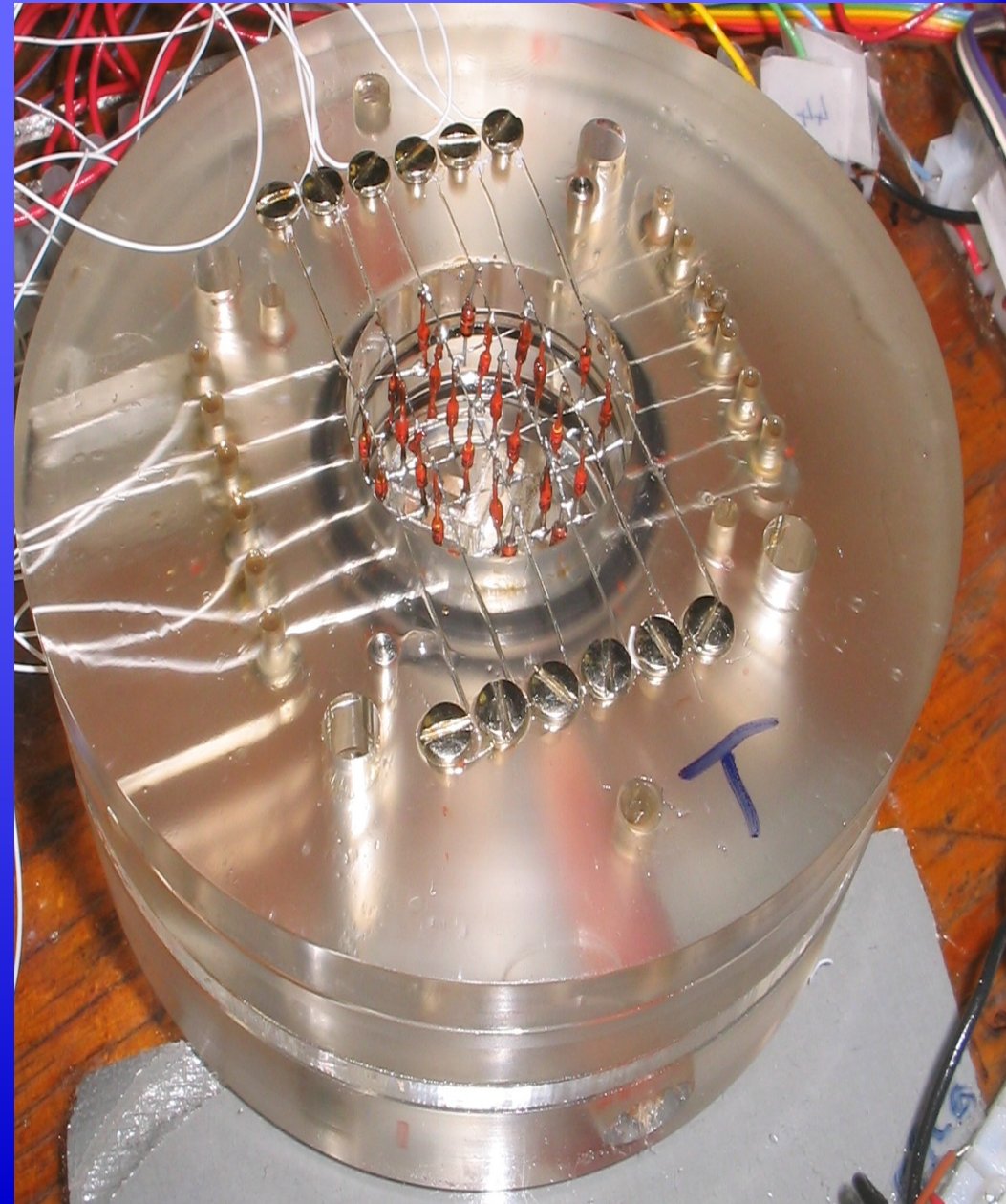
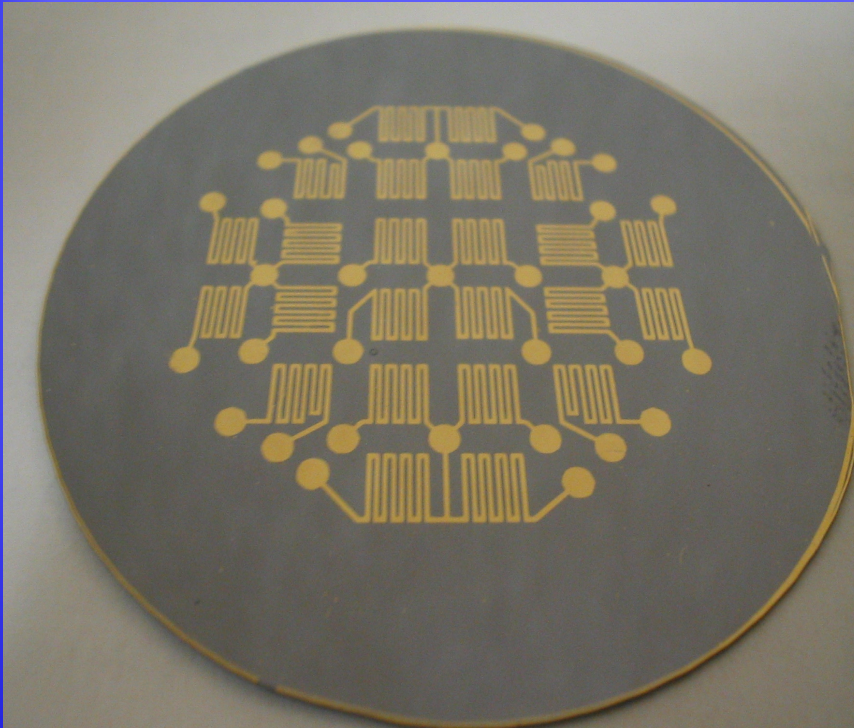


Tang, J., & Bau, H. H., 1993, Stabilization of the No-motion State in Rayleigh-Bénard Convection Through the use of Feedback Control, *Physical Review Letters*, 70, 1795-1798.

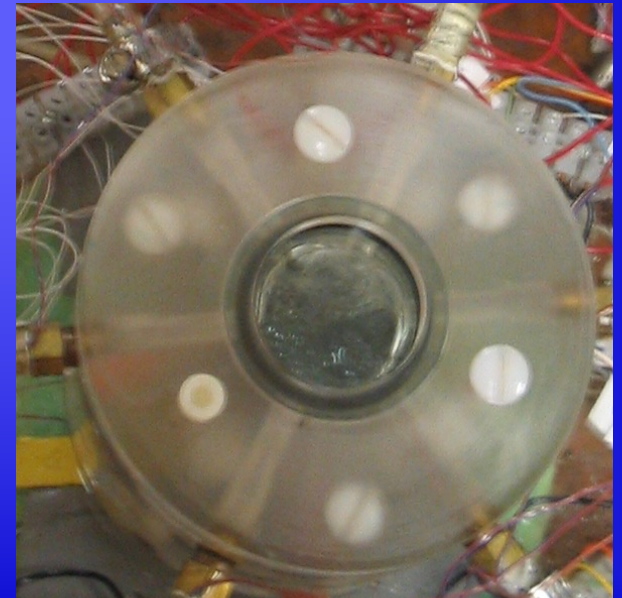
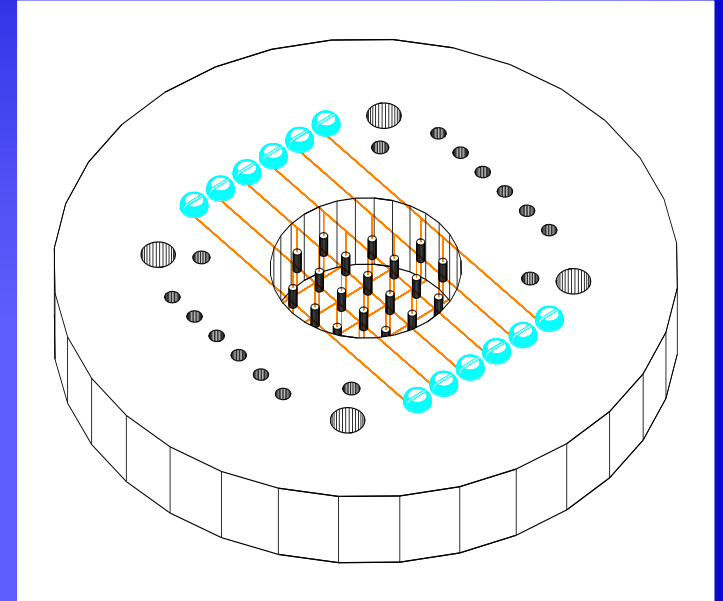
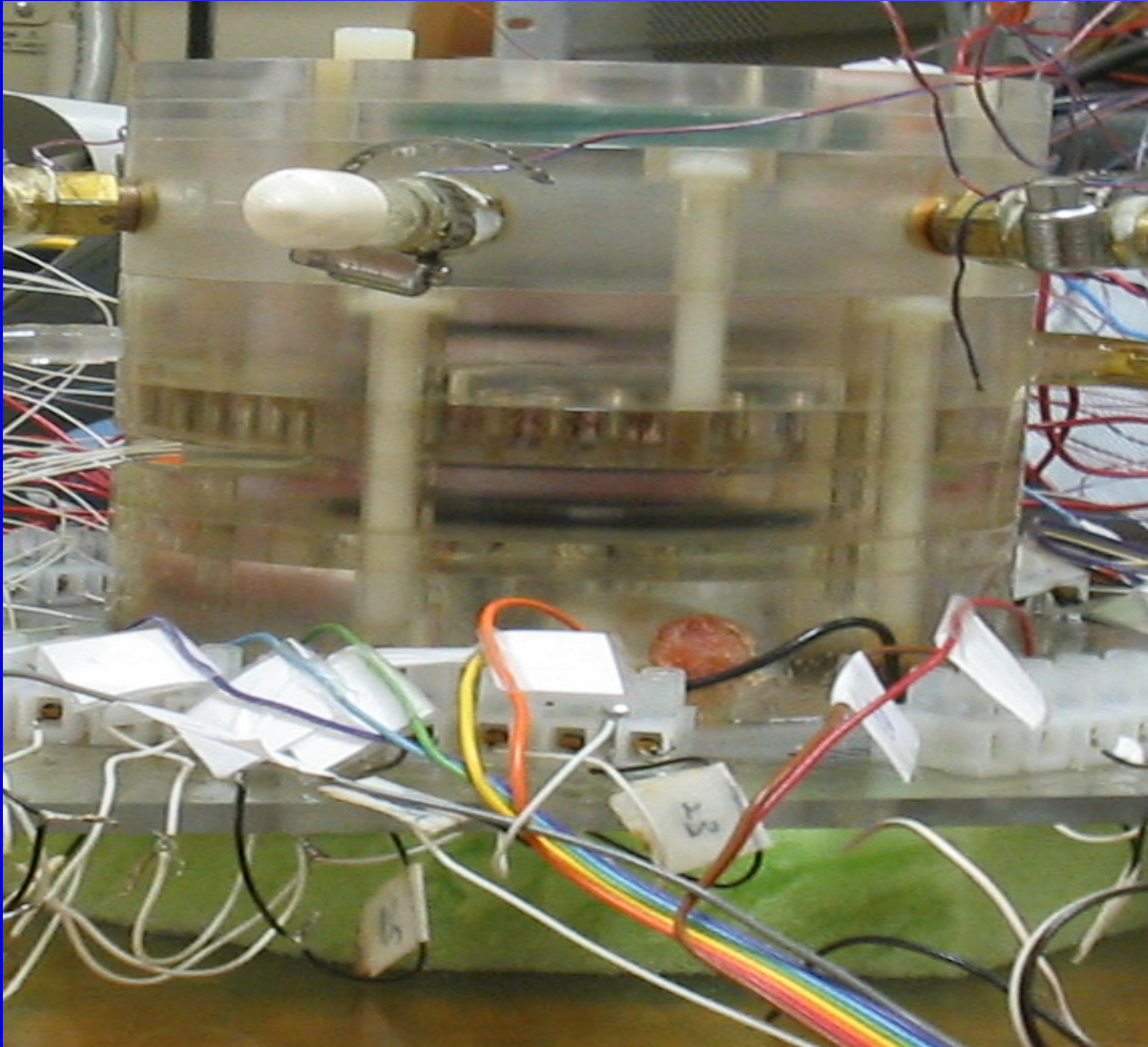
Tang, J., & Bau, H. H., 1993, Feedback Control Stabilization of the No-motion State of a Fluid Confined in a Horizontal, Porous Layer Heated from Below, *J. Fluid Mechanics*, 257, 485-505.

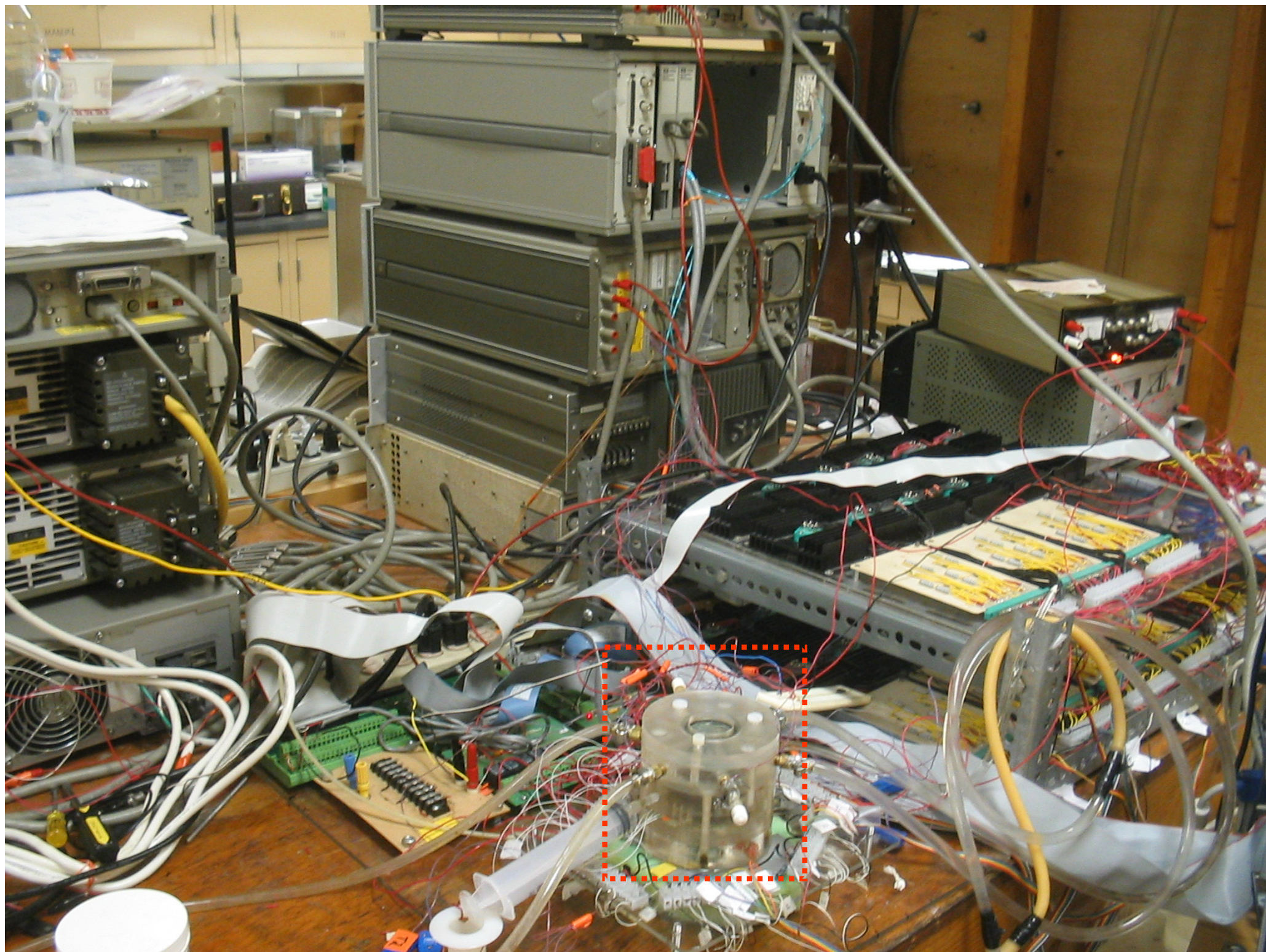
Tang J., and Bau, H. H., 1994, Stabilization of the No-motion State in the Rayleigh-Bénard Problem, *Proceedings Royal Society A*, 447, 587-607.

Experimental Apparatus



An array of diodes for the measurement of the mid-height temperature distribution





PROPORTIONAL-DERIVATIVE CONTROLLER

$$\text{Pr}^{-1} \left(\frac{\partial \vec{u}}{\partial t} + \vec{u} \bullet \nabla \vec{u} \right) = -\nabla P + RaTe_z + \nabla^2 \vec{u}$$

$$\nabla \bullet \vec{u} = 0$$

$$\frac{\partial T}{\partial t} + \vec{u} \bullet \nabla T = \nabla^2 T$$

Controller:

$$\vec{n} \bullet \nabla T \left(r, \phi, -\frac{1}{2}, t \right) = -1 + F(r, \phi, T)$$

General control law:

$$F(r, \phi, T) = \int_D K(r, \phi, z) \theta(r, \phi, z) dV$$

θ is the deviation of the temperature from a desired (set) state

Simplified controller:

$$\vec{n} \bullet \nabla \theta \left(r, \phi, -\frac{1}{2}, t \right) = -k_P \theta(r, \phi, 0, t) + k_D \frac{\partial}{\partial t} \theta(r, \phi, 0, t)$$

LINEAR STABILITY ANALYSIS

$$\text{Pr}^{-1} \frac{\partial}{\partial t} \nabla^2 w = R_q \nabla_1^2 \theta + \nabla^4 w \quad (\text{A1})$$

and

$$\frac{\partial \theta}{\partial t} = w + \nabla^2 \theta, \quad (\text{A2})$$

$$\begin{pmatrix} w \\ \theta \end{pmatrix} = \sum_{n,m,k} \begin{pmatrix} W_{n,m,k} \\ \Theta_{n,m,k} \end{pmatrix} (z) f_{n,m,k}(r, \varphi) \exp(\sigma_{n,m,k} t)$$

$$\nabla_1^2 f + \lambda^2 f = 0$$

$$((D^2 - \lambda^2)(D^2 - \lambda^2 - \sigma)(D^2 - \lambda^2 - \text{Pr}^{-1}\sigma) + \lambda^2 R_q) \Theta = 0$$

$$\Theta(z) = \sum_{i=1}^3 (A_i \cosh(x_i z) + A_{i+3} \sinh(x_i z))$$

$$\theta(x, y, -\frac{1}{2}) = C(\theta_0) = -K_p \theta_0,$$

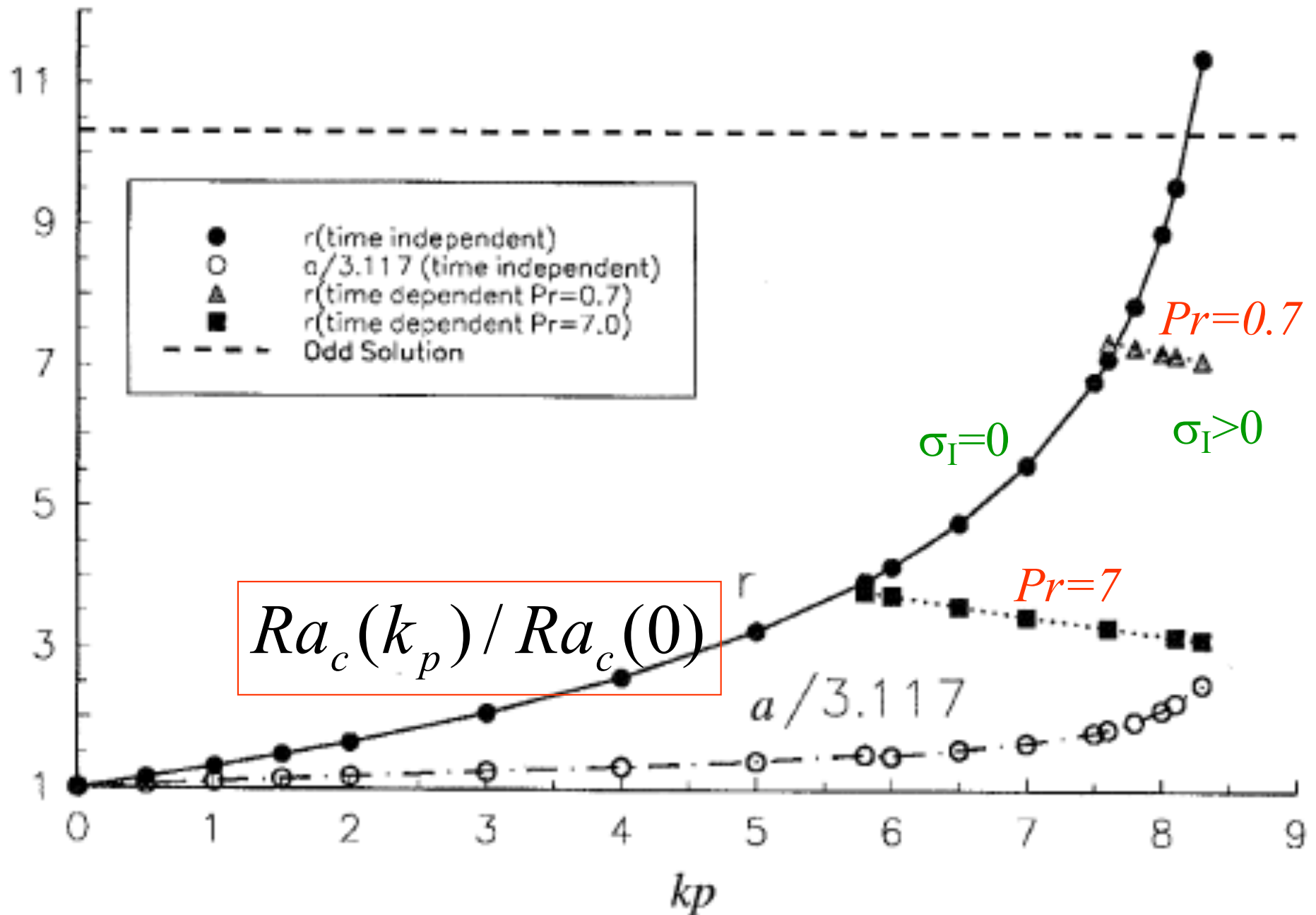
$$D_\theta = \det \begin{bmatrix} M_\theta & A_\theta \\ \mathbf{0} & N_\theta \end{bmatrix} = 0.$$

$$N_\theta = \begin{pmatrix} \mu + \cosh \frac{1}{2}x_1 & \mu + \cosh \frac{1}{2}x_2 & \mu + \cosh \frac{1}{2}x_3 \\ \xi + \chi_1 \cosh \frac{1}{2}x_1 & \xi + \chi_2 \cosh \frac{1}{2}x_2 & \xi + \chi_3 \cosh \frac{1}{2}x_3 \\ \zeta_1 \sinh \frac{1}{2}x_1 & \zeta_2 \sinh \frac{1}{2}x_2 & \zeta_3 \sinh \frac{1}{2}x_3 \end{pmatrix}$$

$$M_\theta = \begin{pmatrix} \sinh \frac{1}{2}x_1 & \sinh \frac{1}{2}x_2 & \sinh \frac{1}{2}x_3 \\ \chi_1 \sinh \frac{1}{2}x_1 & \chi_2 \sinh \frac{1}{2}x_2 & \chi_3 \sinh \frac{1}{2}x_3 \\ \zeta_1 \cosh \frac{1}{2}x_1 & \zeta_2 \cosh \frac{1}{2}x_2 & \zeta_3 \cosh \frac{1}{2}x_3 \end{pmatrix}$$

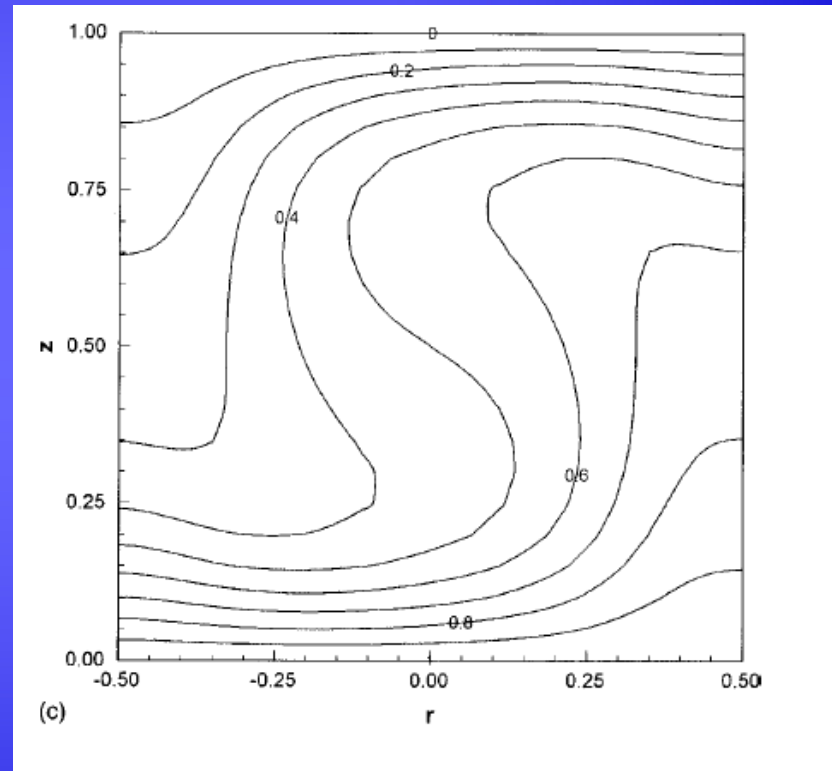
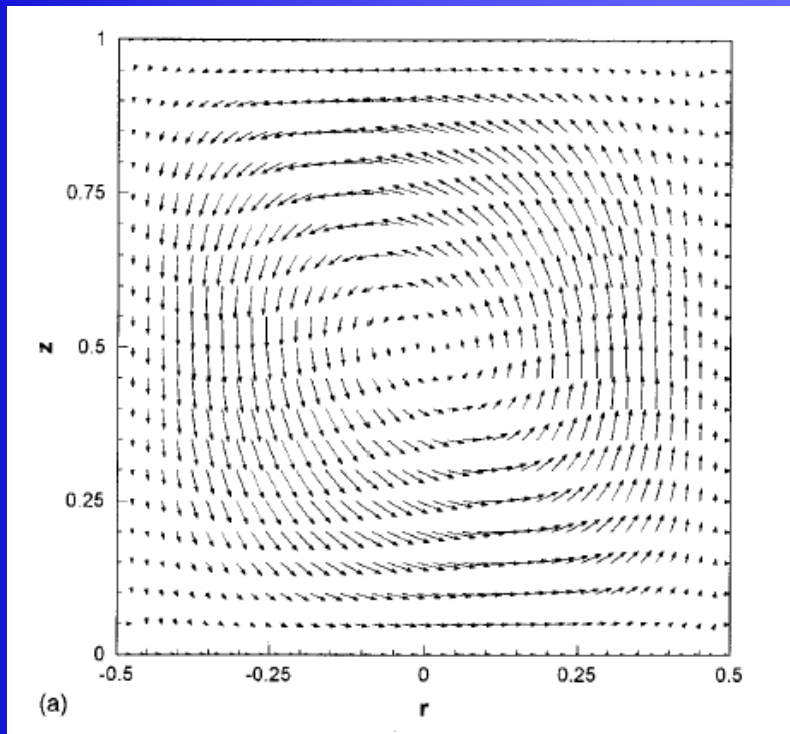
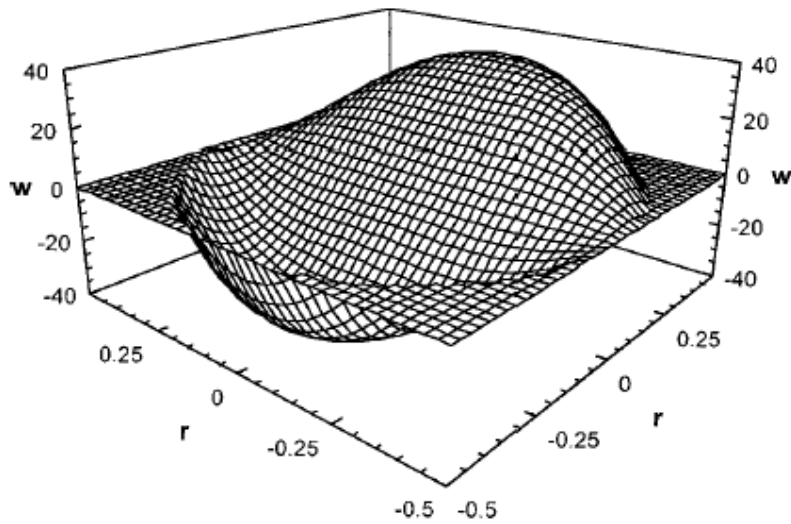
$$\chi_i = (x_i^2 - a^2 - \sigma); \quad \zeta_i = x_i \chi_i; \quad \mu = \frac{1}{2}K_p; \quad \xi = 0;$$

PROPORTIONAL CONTROLLER – STABILITY CURVE



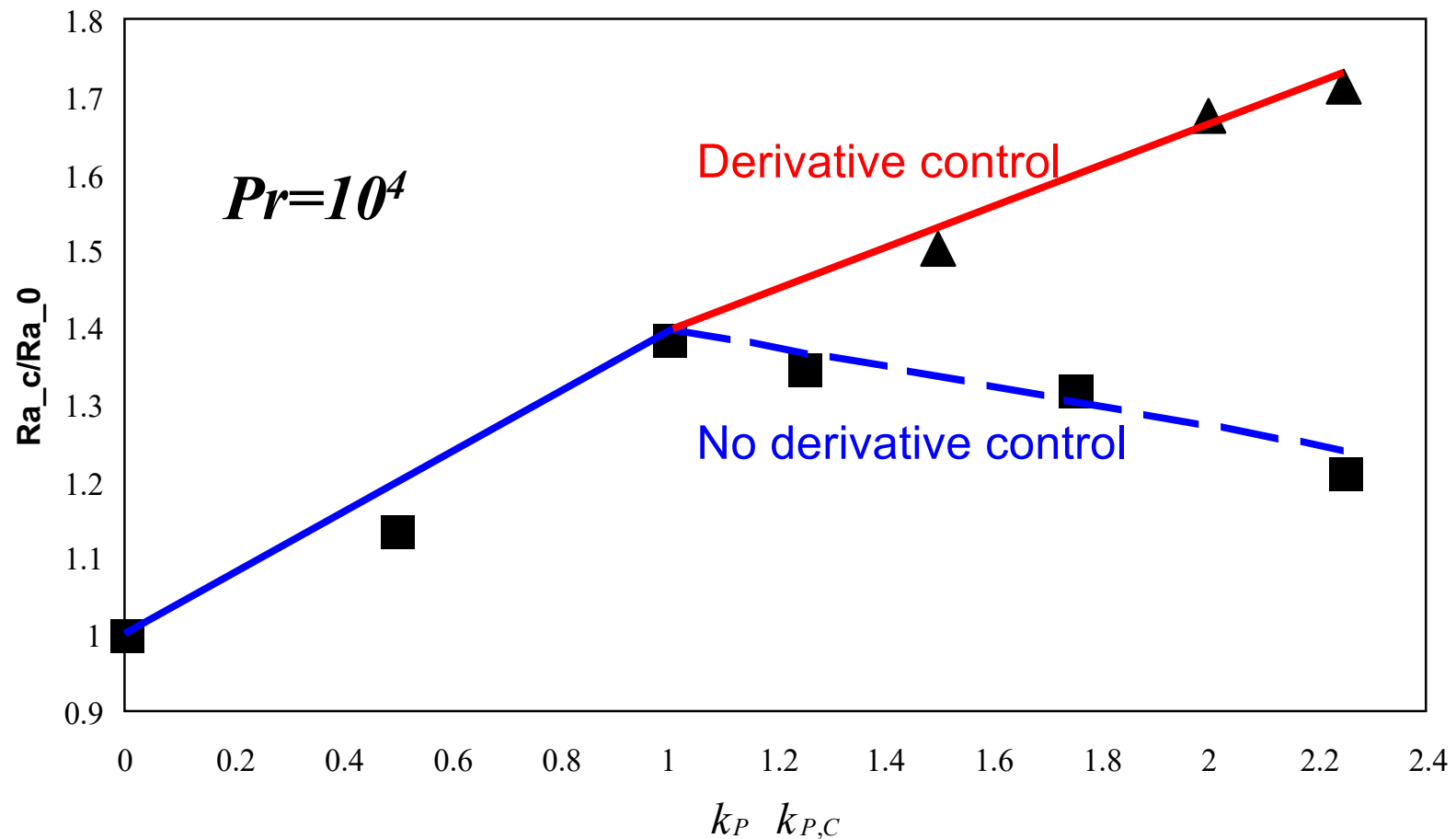
THE UNCONTROLLED FLOW IN THE CYLINDER

ASPECT RATIO: $H/D=1$



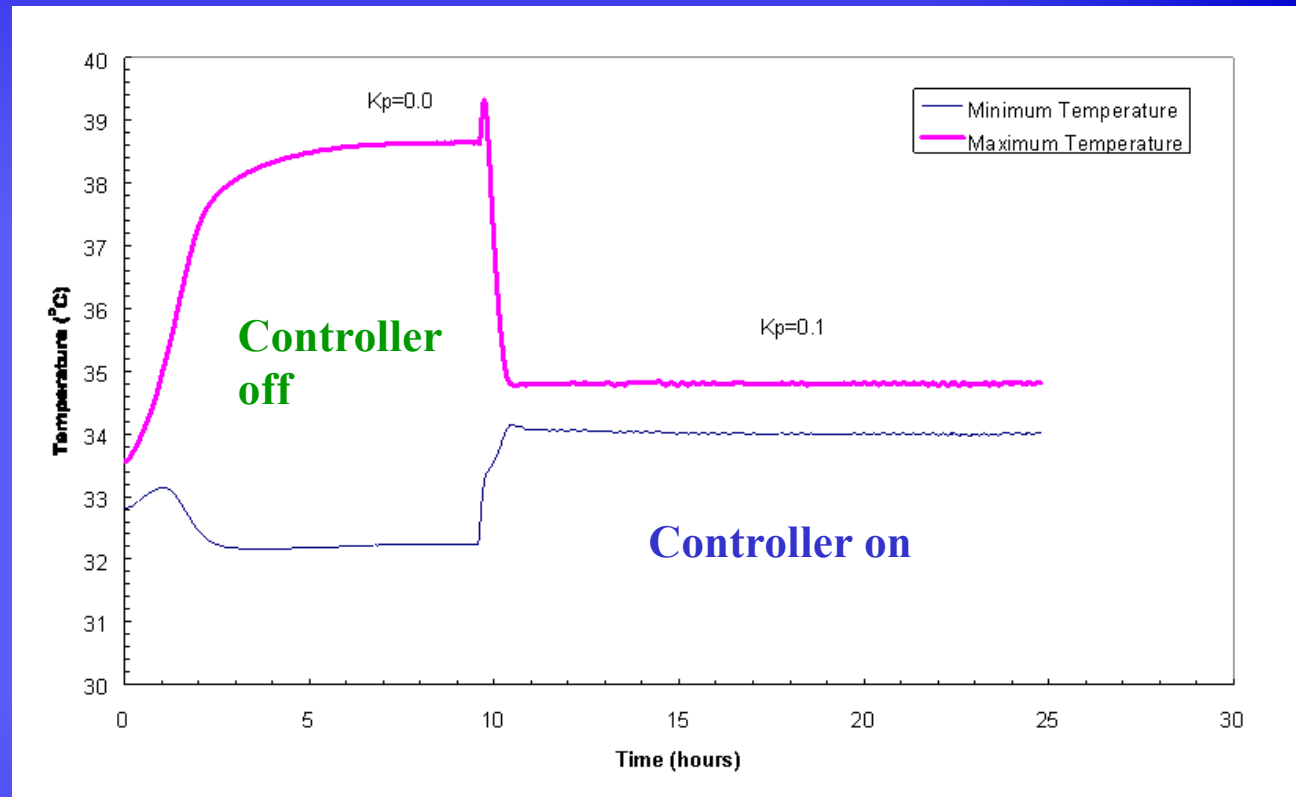
The performance of the proportional and proportional derivative controller

$$\vec{n} \cdot \nabla \theta \left(r, \phi, -\frac{1}{2}, t \right) = -k_P \theta(r, \phi, 0, t) + k_D \frac{\partial}{\partial t} \theta(r, \phi, 0, t)$$



DYNAMICS OF THE CONTROLLED SYSTEM

- Measured maximum and minimum mid-height temperatures in an upright circular cylinder are depicted as functions of time. Initially, the controller is not active. When the bottom heating is turned on, convection is established. Once the controller is turned on, the difference between the maximum and minimum temperatures decreases and the convection is suppressed. The controller does not change the power input into the cylinder.



$Pr=10,000$

Summary

- **The proportional controller and proportional-derivative controller were successfully implemented both in experiment and theory**
- **The proportional controller increased the Rayleigh number by a factor of 1.4**
- **Further increases in the proportional controller gain led to a decrease in the critical Rayleigh number, due to oscillations in the presence of large proportional gain**
- **A combination of proportional and derivative controllers was able to increase the critical Rayleigh number by as much as a factor of 1.7.**

QUESTIONS

Can we do better with synthesized (optimal controllers such as H_2 and H_∞)?

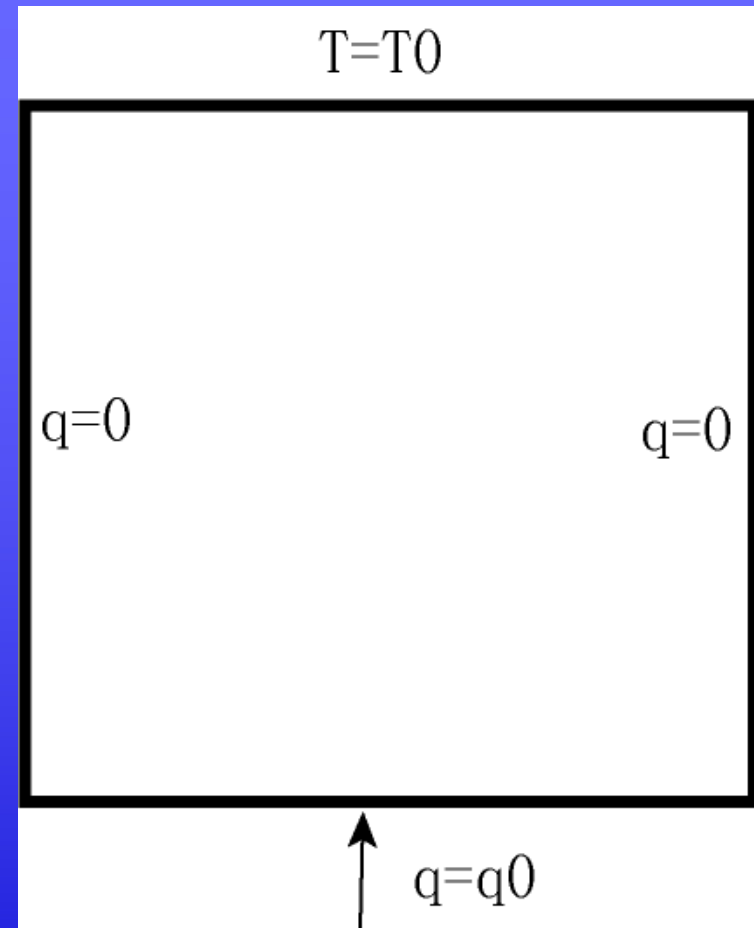
What is the effect of the nonlinear terms that are neglected in the controller's design?

What is the basin of attraction of the controlled system?

To investigate the above issues, we selected a relatively simple model problem: The *Rayleigh-Benard-Lapwood (RBL)* convection of a box saturated with a porous medium, heated from below and cooled from above.

The Darcy-Lapwood-Rayleigh-Benard (DLRB) Problem

- Two-dimensional, square box, with edge length H , filled with a saturated porous medium.
- The box is heated from below with a controllable heat flux.
- The box's top is maintained at a uniform temperature T_0 .
- The left and right walls are insulated



Mathematical model

- Continuity equation:

$$\nabla \cdot \vec{V} = 0,$$

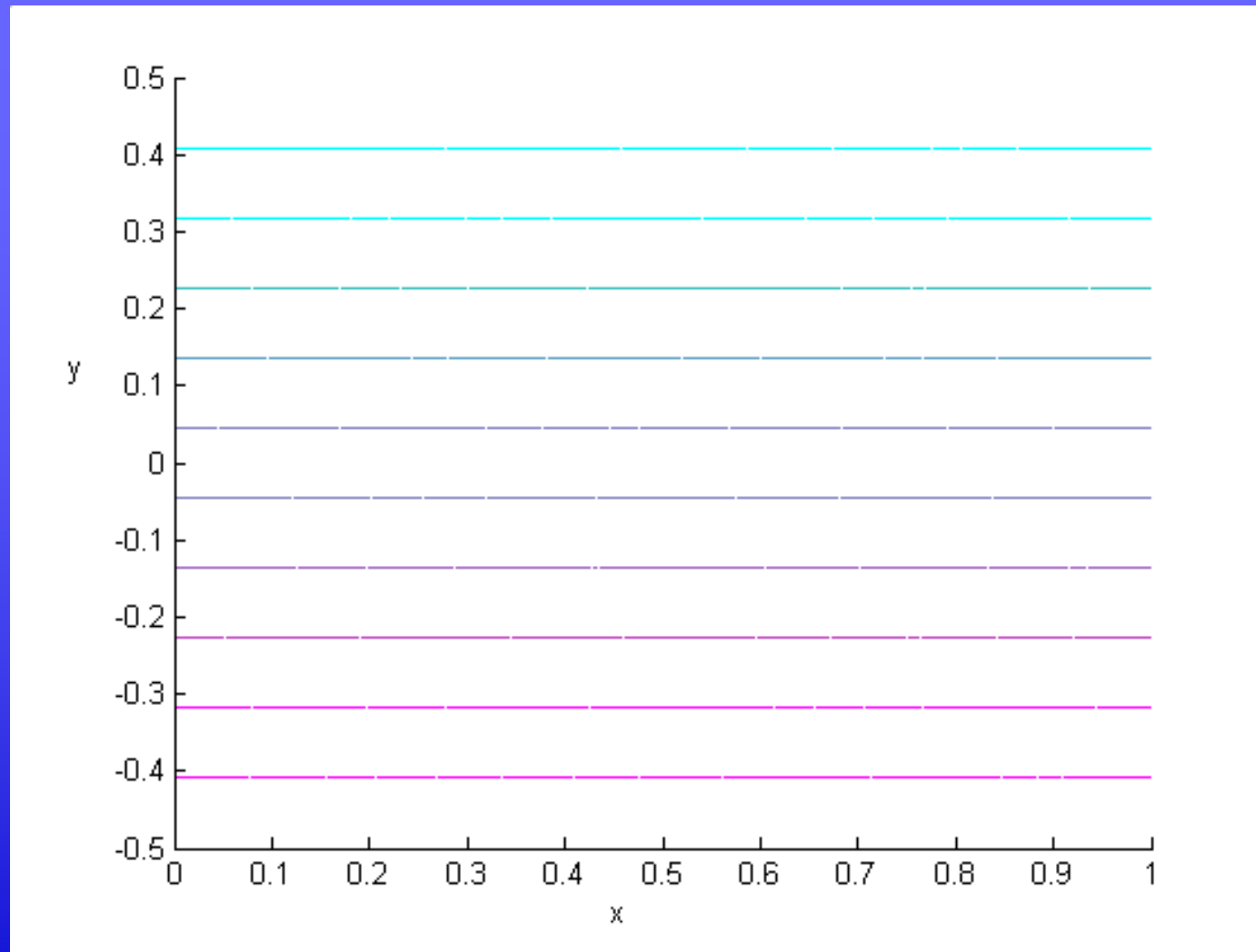
- Momentum equation:

$$\vec{V} = -\nabla P + RaTe_y$$

- Energy equation:

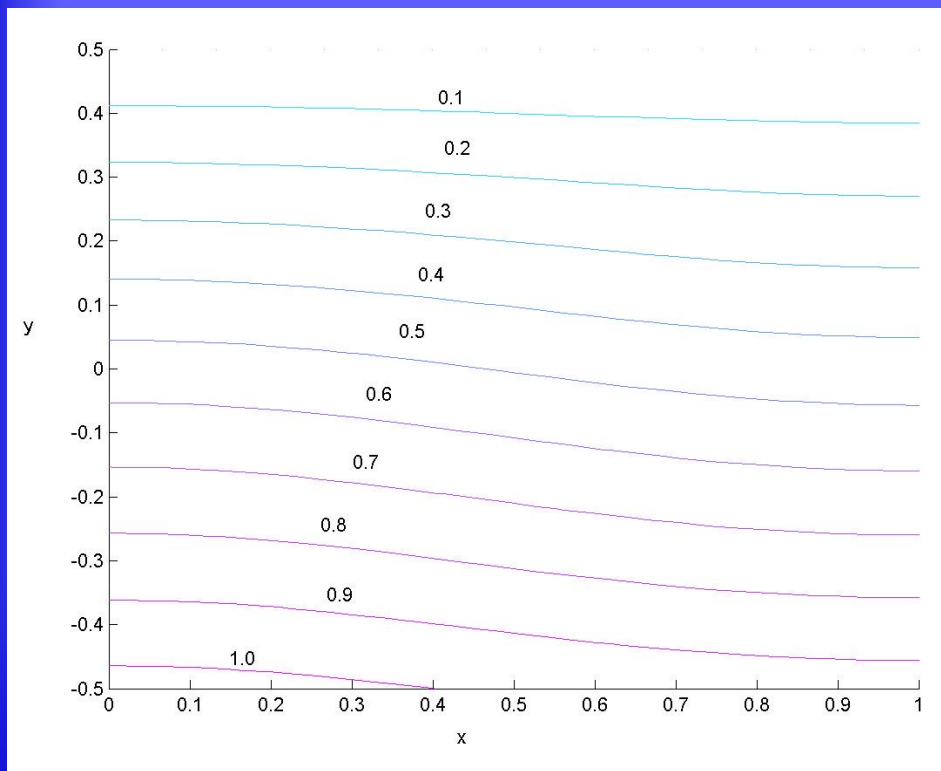
$$\chi \frac{\partial T}{\partial t} + \vec{V} \cdot \nabla T = \nabla^2 T$$

Temperature distribution (no-motion state)

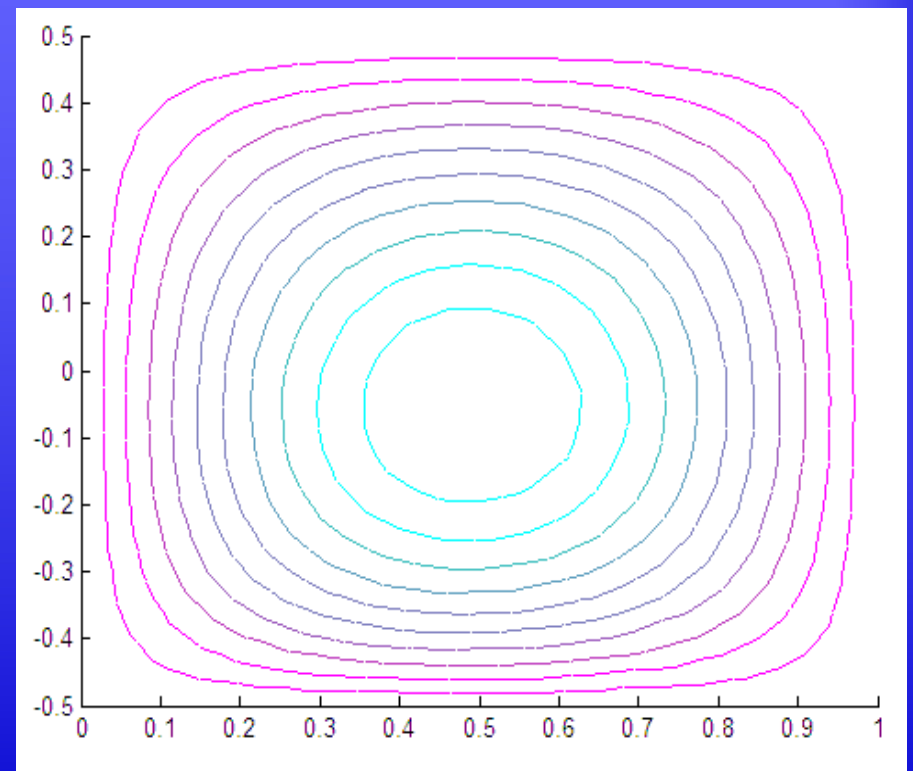


Convection at $Ra=30$

Constant temperature
contour



Streamlines



Linear model

- The linearized form of the equations in local form about the motionless state $\vec{V} = 0$ $T = 0.5 - y$

$$\chi \frac{\partial}{\partial t} \theta = \nabla^2 \theta + v_y,$$

$$\nabla^2 v_y = Ra \frac{\partial^2 \theta}{\partial x^2}.$$

Discretized Linear Model

- The PDEs are converted into a set of ordinary differential equations by projection on a finite element space

$$\chi D_a \dot{\Theta} = -K_2 \Theta + Lq + C_1 V_y,$$

$$K_1 V_y = Ra P_1 \Theta$$

- To verify the numerical code, the computed critical Rayleigh numbers for the uncontrolled problem (Neuman boundary condition) and for the related problem of fixed bottom temperature (Dirichlet boundary condition) were, respectively, 29.3 and 37.1. These are in excellent agreement with published data

Plant and Observer Equations

- By eliminating V_y in favor of θ :

$$\dot{X}(t) = A(Ra)X(t) + B_u U(t) + B_w w(t)$$

$$Y(t) = CX(t)$$

- Controller objective: stabilize the no-motion, equilibrium state at high Ra numbers

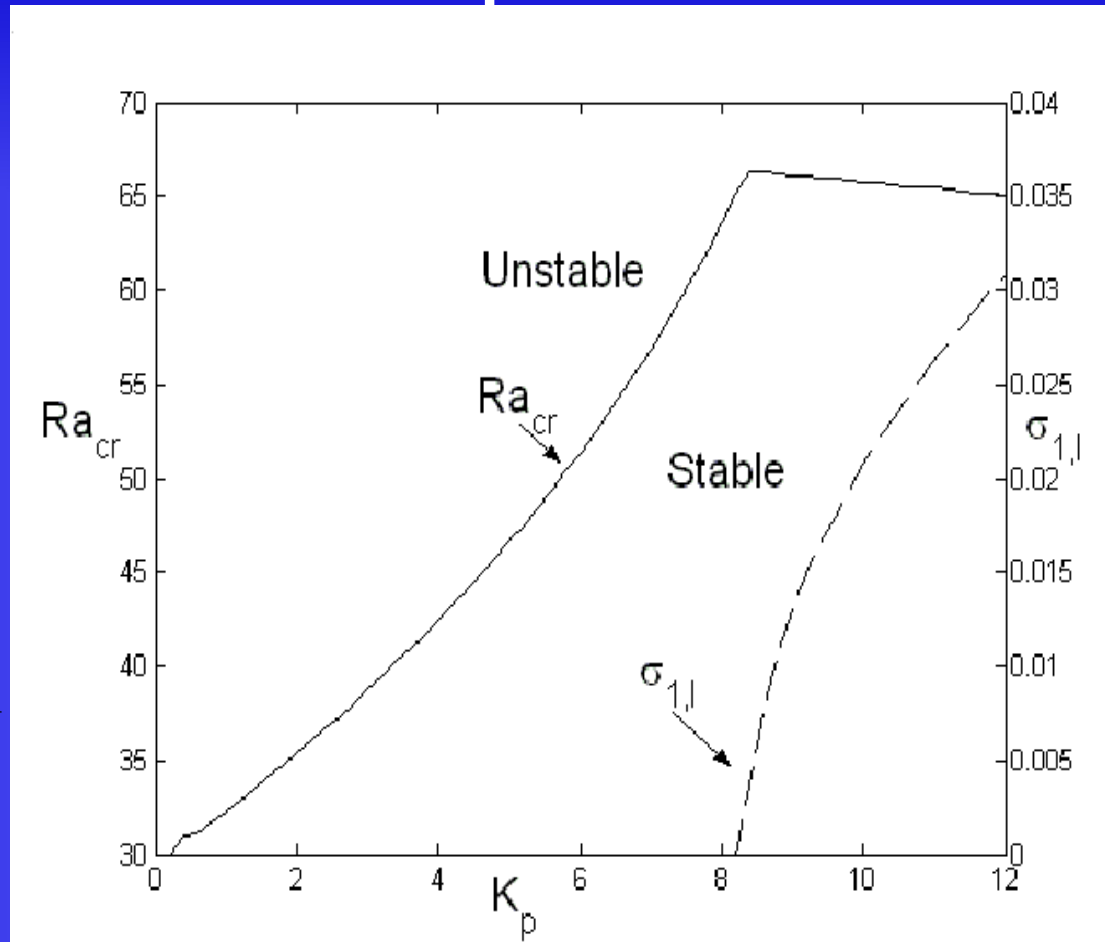
Ad-Hoc Proportional Controller

- The proportional controller:

$$U = -K_p X(x, 0, t)$$

- The control input (the heat flux at $y=-0.5$) is modulated in proportion to the deviation of the mid-layer temperature from its conductive value

Ad-hoc Proportional Controller



$Ra_{\text{uncontrolled}}$
 $=29.3$

The critical Rayleigh number (solid line) for the transition from the motionless to the motion state and the corresponding imaginary part σ_I of the eigenvalue (dashed line) are depicted as functions of the ad-hoc proportional controller gain K_p .

Proportional controller's performance

- As K_p increases, the critical Rayleigh number increases as well. When $K_p=8.4$, the critical Rayleigh number is about 66.8
- Further increases in the controller's gain lead to oscillatory convection and reduce the critical Rayleigh number

H_2 Controller

- The cost function:

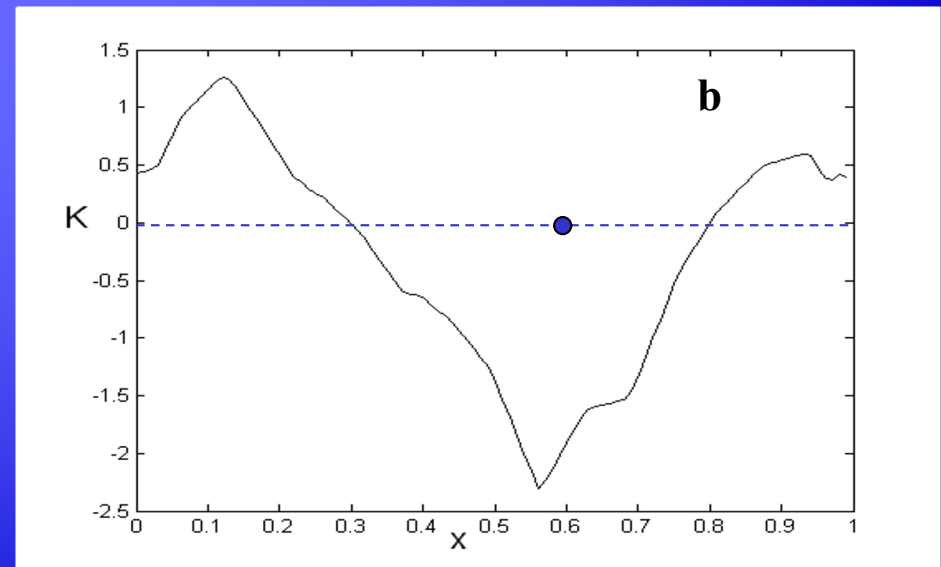
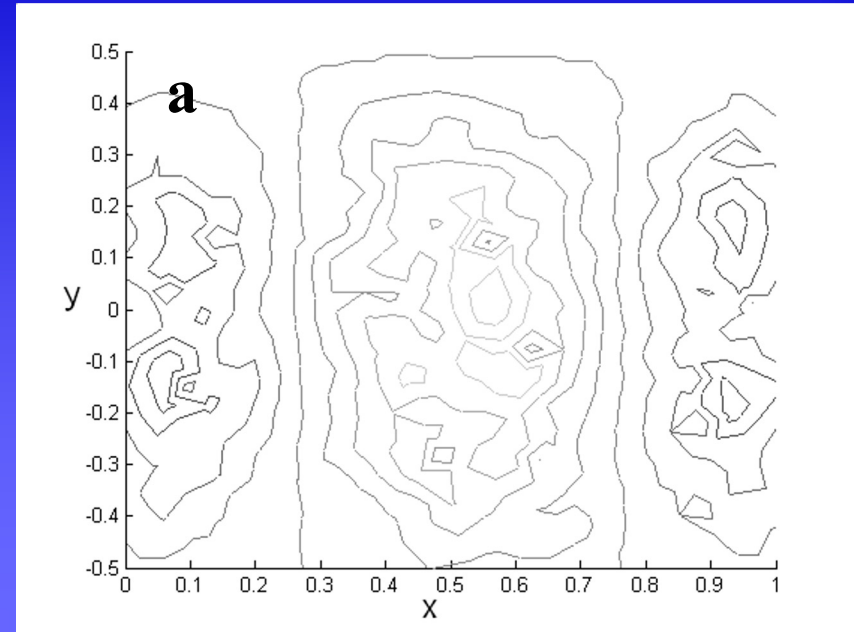
$$J(X(t), U(t)) = \lim_{t_f \rightarrow \infty} \frac{1}{t_f} \int_0^{t_f} (X^T Q X + l^2 U^T R U) dt$$

- The control strategy is:

$$U(t) = -l^{-1} R^{-1} B_u^T P X(t) = -K X(t)$$

$$\frac{dP}{dt} = PA + A^T P - PB_u B_u^T P + Q$$

- Contours of the H_2 controller gain associated with an actuator located at $x=0.6$ are depicted as a function of location (a) and $K(x,0)$ as a function of x (b). The controller is designed to operate at $Ra_D=120$.
- The gain is not local



H_∞ Controller (Robust Controller)

- H_∞ controller stabilizes the system under the worst possible disturbance.
- It requires that the following transfer function is bounded

$$\sup_{w(t)} \frac{\|Z(t)\|_2}{\|w(t)\|_2} < \gamma$$

$$\|Z(t)\|_2^2 = \int_0^{+\infty} X^T(t) Q X(t) dt$$

- The above is equivalent to finding the saddle point of the objective function

$$J_1 = \|Z(t)\|_2^2 - \gamma^2 \|w(t)\|_2^2 + l^2 \|U(t)\|_2^2$$

Calculation of the controller's gain

$$u(t) = -B_u^T P x(t) = -K x(t)$$

- P is obtained by solving the Riccati equation

$$PA + A^T P - P(B_u B_u^T - \gamma^{-2} B_w B_w^T)P + C^T C = 0$$

Constructing a H_2 state estimator

- Only some of the states are measured

$$m(t) = C_m x + D_w w$$

- By minimizing the error between the observed states and real states, the estimator will be

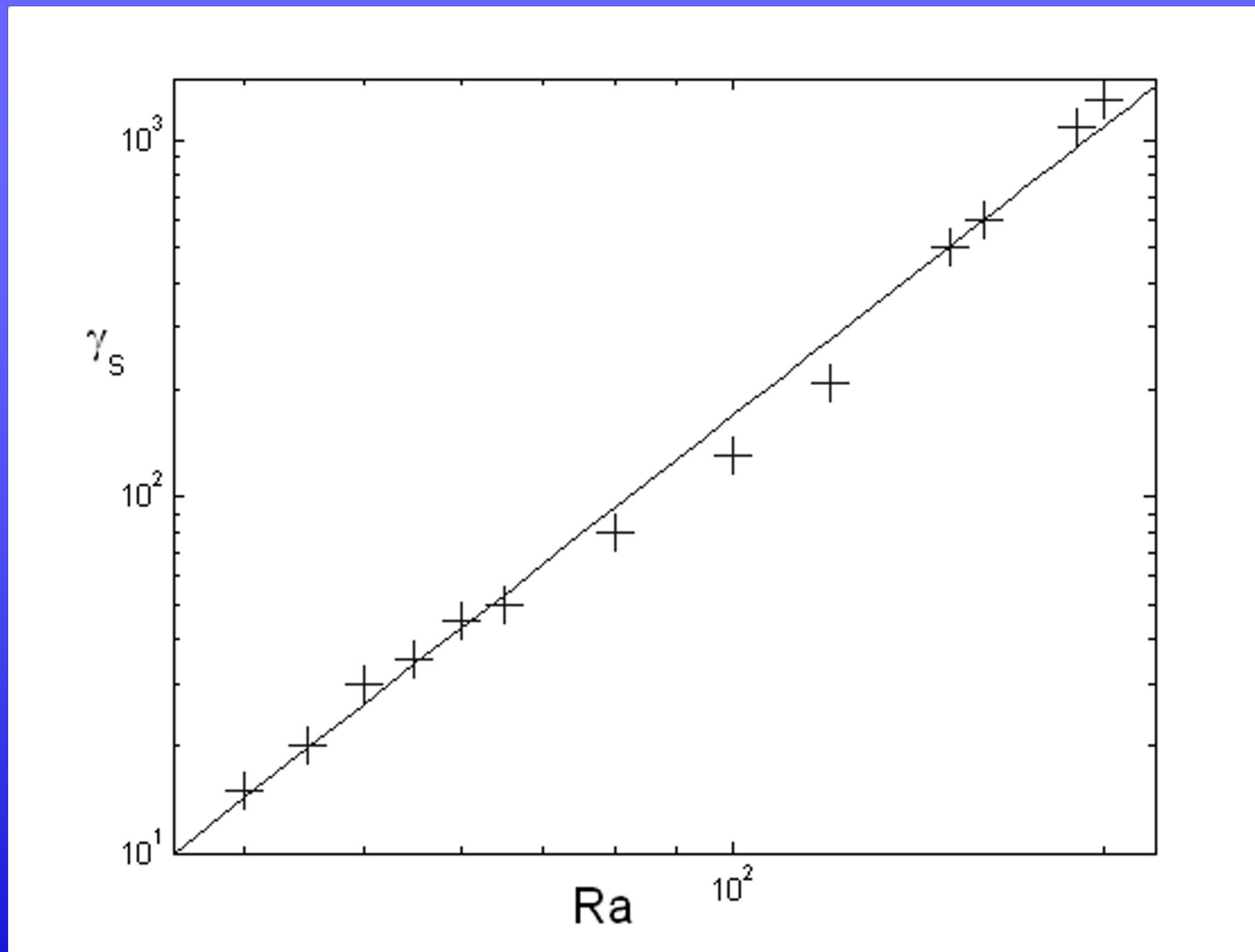
$$\dot{\hat{x}}(t) = [A + \gamma^{-2} B_w B_w^T P - B_u B_u^T P - Q_m C_m^T C_m] \hat{x}(t) + Q_m C_m^T m(t)$$

$$AQ + QA^T - Q(C_m^T C_m - \gamma^{-2} C^T C)Q + B_w B_w^T = 0$$

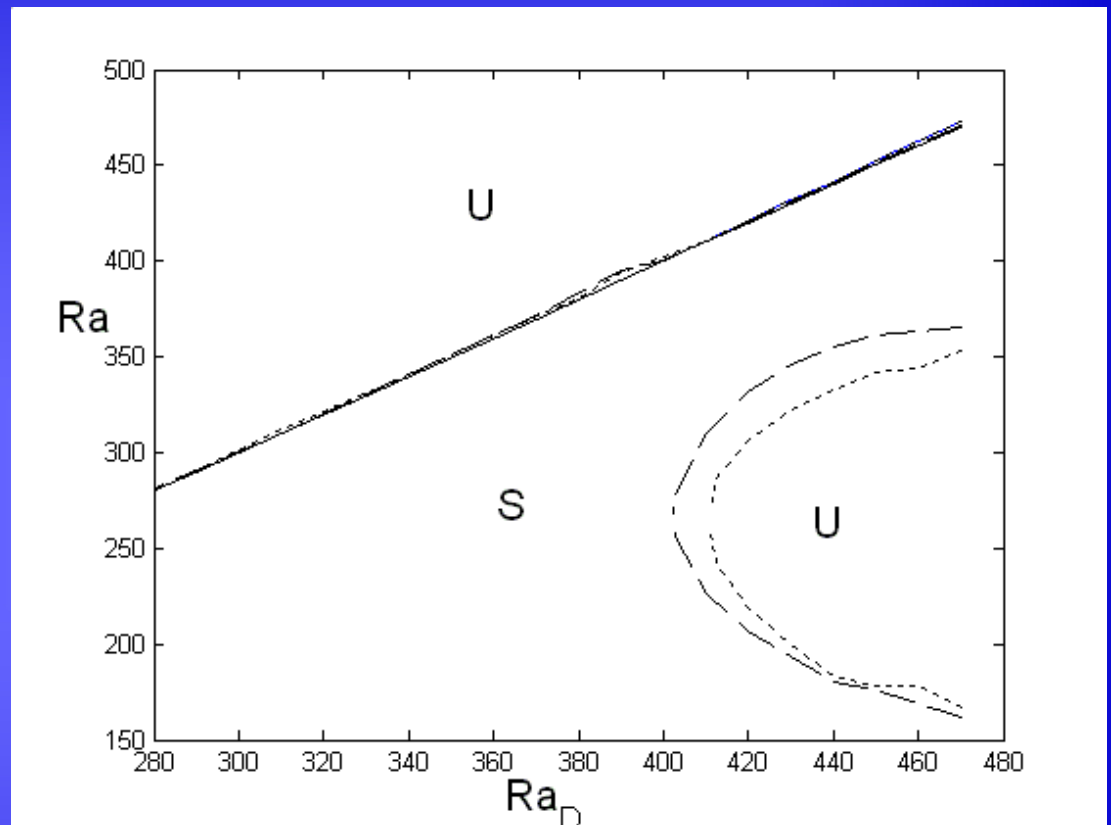
Selection of γ

- In general, the smaller γ , the better the performance
- γ needs to satisfy the following conditions:
 1. The real parts of the eigenvalues of the matrix $A - (B_u B_u^T - \gamma^{-2} B_w B_w^T) P$ must be negative.
 2. The real parts of the eigenvalues of matrix $A - Q(C_m^T C_m - \gamma^{-2} C_T C)$ must be negative.
 3. The spectral radius $\rho(PQ) < \gamma^2$.

The smallest bound γ_c of the transfer function for which a steady solution of the Riccati equation exists as a function of the Rayleigh number



The range of Rayleigh numbers for which the controlled system is stable as a function of the Rayleigh number for which the controller was designed (Ra_D). The solid line depicts the design Rayleigh number. The dashed and dotted lines correspond, respectively, to the linear, quadratic Gaussian (H_2) controller and the suboptimal robust controller. The regions of stability and instability are indicated in the figure with the letters S and U, respectively.



The Performance of H_2 controller and H_∞ robust controller

- Both controllers can stabilize the system at any desired Ra number
- Due to the large γ , the differences between H_2 controller H_∞ and controller are slight
- Both controllers maintain linear stability for all $Ra < Ra_D$ only when Ra_D is smaller than a certain Ra
- As Ra number increases, the stable range shrinks.

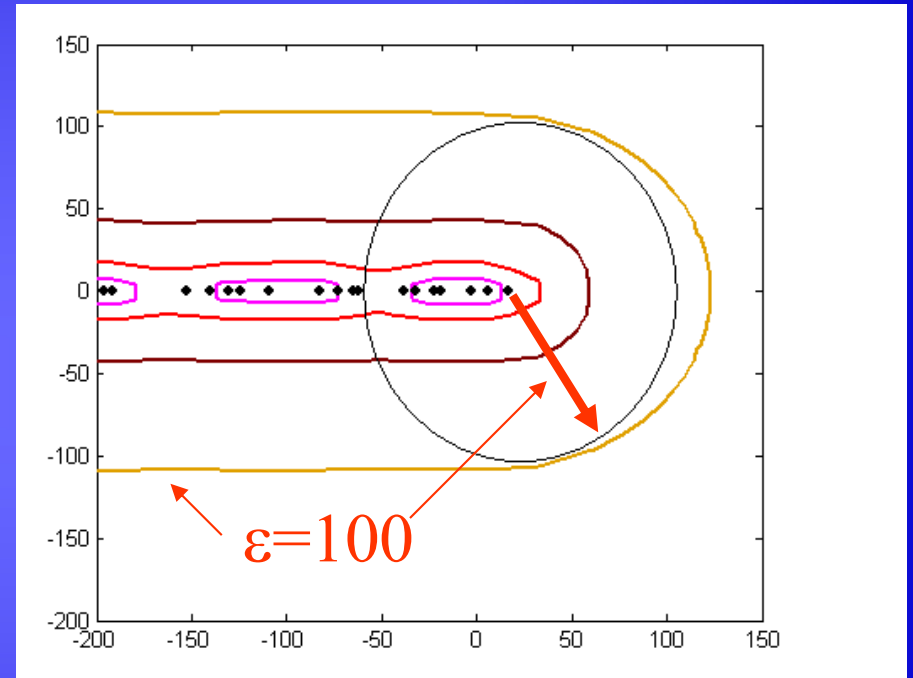
The Normality of the Linear Operator

- When a stable system is normal, all disturbances will decay monotonically
- When the controlled system's linear operator is not normal, some disturbances may amplify (sometimes a great deal) before their eventual decay (even when all the eigenvalues have a negative real part)
- Large disturbances may render the neglected nonlinear terms important, thus providing a bypass mechanism for transition from the stabilized state to another state.
- Pseudospectra and transient growth characterize the non-normality

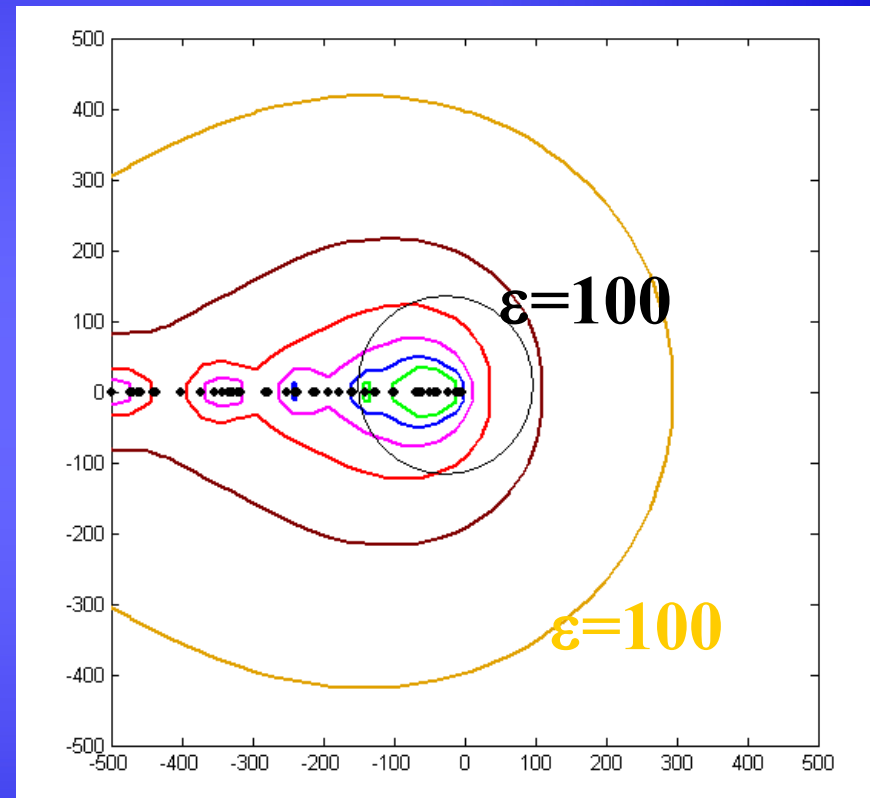
Linear operator's pseudospectra

- The linear operator of the controlled system: Ac .
- ΔAc is a perturbation to Ac
- The ε -pseudospectra of Ac , $\Delta(Ac, \varepsilon)$, is the set of eigenvalues z_ε of $Ac + \Delta Ac$, where $\|\Delta Ac\| = \|\varepsilon Ac\|$.
- When Ac is normal, $\Delta(Ac, \varepsilon)$ is a set of points within a distance ε from the corresponding points in $\Delta(Ac, 0)$.
- When Ac is non-normal, the distance between points in $\Delta(Ac, \varepsilon)$ and the corresponding points in $\Delta(Ac, 0)$ will be much larger than ε .

- The pseudospectra of the linear operator A of the uncontrolled system when $Ra=66$. The contour lines correspond to $\varepsilon=1, 10^{1/2}, 10, 10^{3/2},$ and 10^2 . The disk has a radius of 100. A is nearly normal



- The pseudospectra of the linear operator A_c of the system controlled with a H_2 controller when $Ra=120$. The contour lines correspond to $\varepsilon=1, 10^{1/2}, 10, 10^{3/2},$ and 10^2 . The disk has a radius of 100.
- The operator A_c is nonnormal



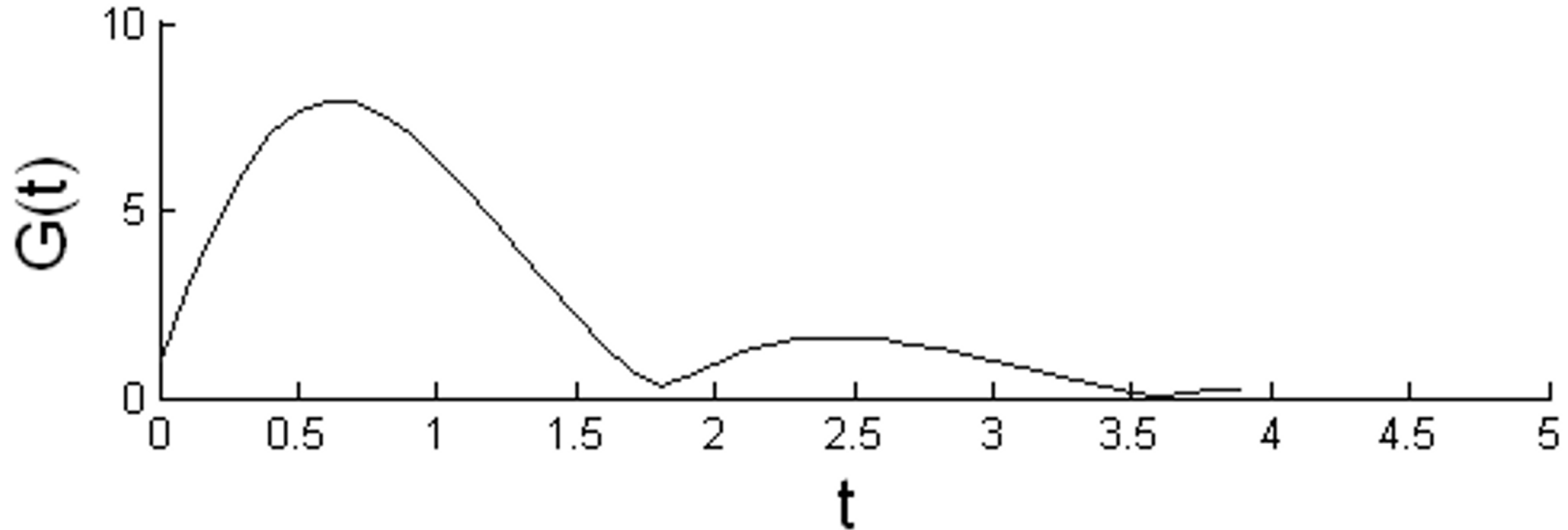
Transient growth

- The linear, controlled system has a solution of the form

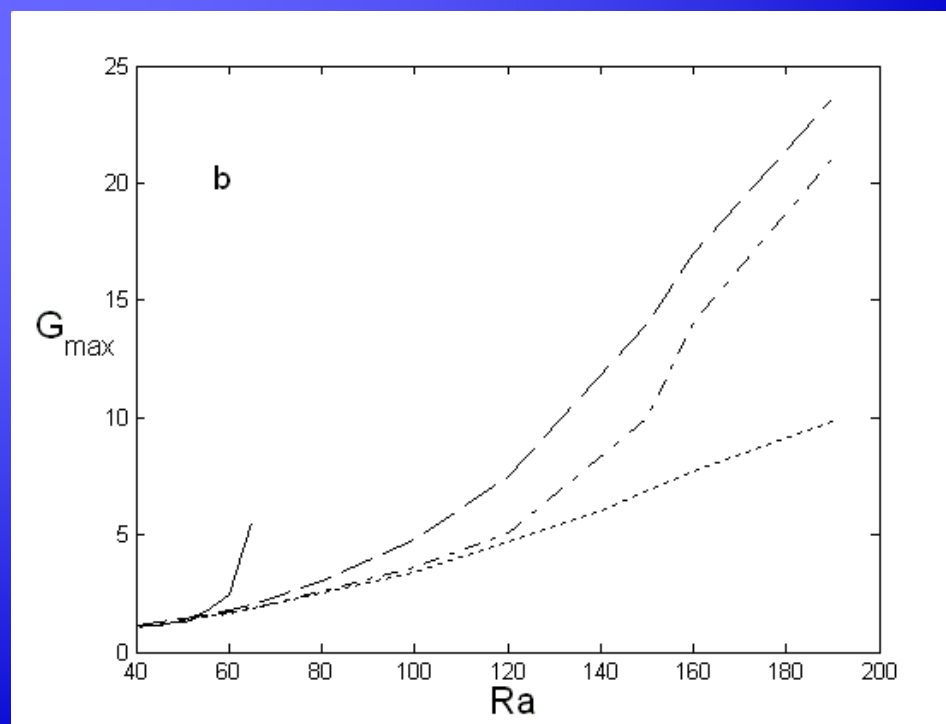
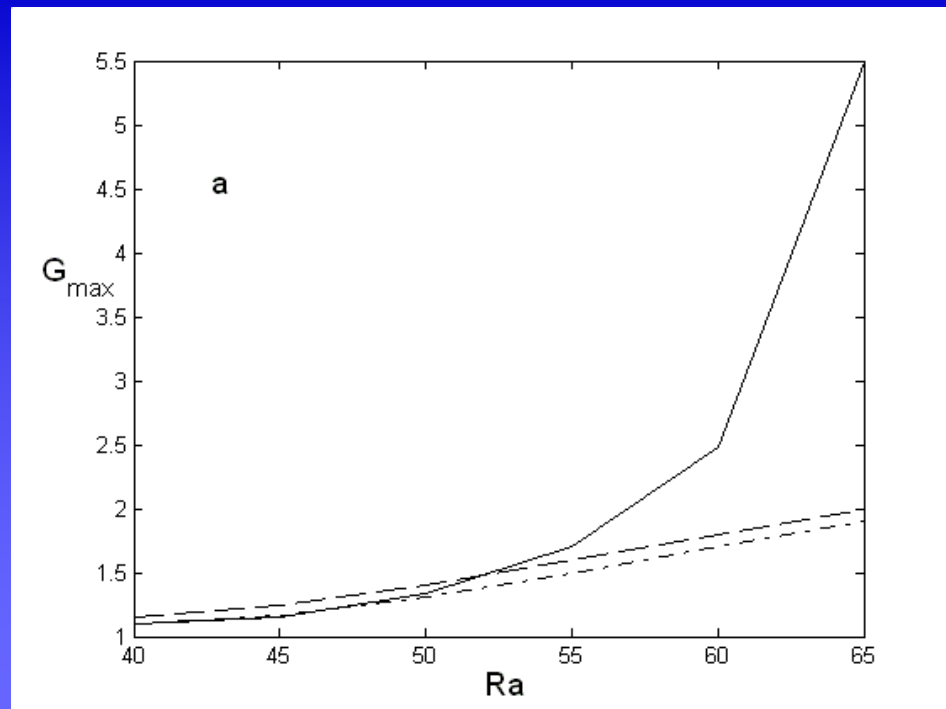
$$X(t) = \exp[(A - BK)t]X(0)$$

- $\|x(t)\| = \|\exp[(A - BK)t]\| \|x(0)\|$, where $\|x(t)\|^2 = X^T(t) \cdot x(t)$.
- $G(t) = \|\exp[(A - BK)t]\|$ is a measure of the disturbance's growth
- The maximum value of $G(t)$, $G_{max} = \max_{0 \leq t \leq \infty} G(t)$ is a measure of the disturbance's amplification

**The transient growth of $G(t)$ as a function of time.
Ad-hoc, proportional controller, $R_a=66$, and $K_p=8.4$.**



- The maximum transient growth G_{\max} as a function of the Rayleigh number for the various control strategies. The solid, dashed, dash-dot and dotted lines correspond, respectively, to the ad-hoc proportional (with gain $K_p=8.4$) controller, quadratic-Gaussian (H_2) controller, suboptimal robust controller, and H_2 controller without estimator.



Dynamics of the Nonlinear Controlled System

- The most dangerous disturbance which leads to the largest amplification, is used as initial condition to the nonlinear simulation
- The basin of attraction can be determined numerically
- Finite element method is used to solve the Lapwood problem

Determining most dangerous disturbance

- Singular value decomposition allows us to determine this “most dangerous” disturbance

$$U^H \exp(A_c t_{\max}) V = \Sigma$$

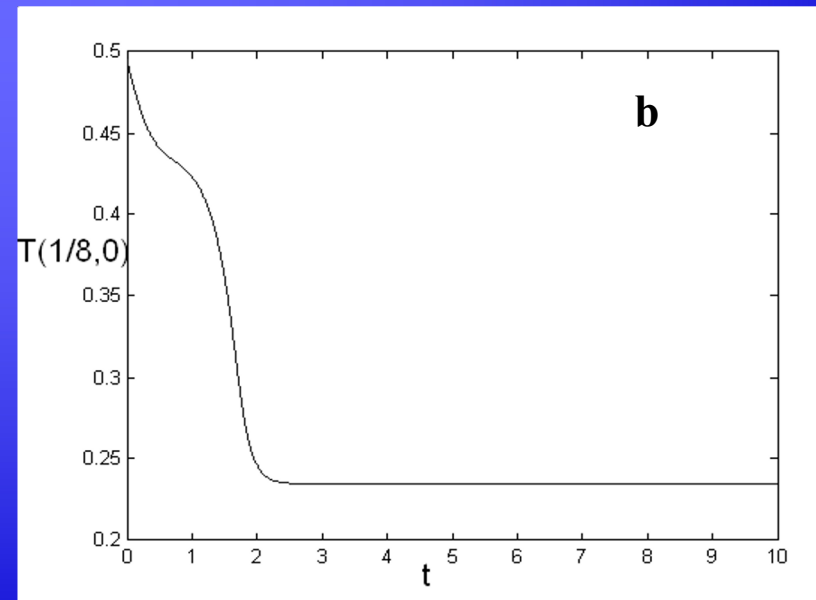
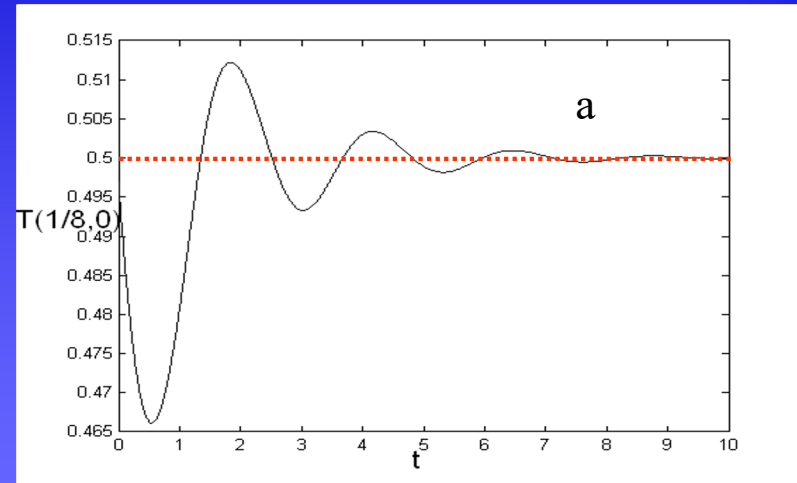
- U and V are unitary matrices with orthogonal columns ($UU^H = V^H V = I$) and Σ is a diagonal matrix that contains the singular values

$$\exp(A_c t_{\max}) V_1 = U_1 \sigma_1$$

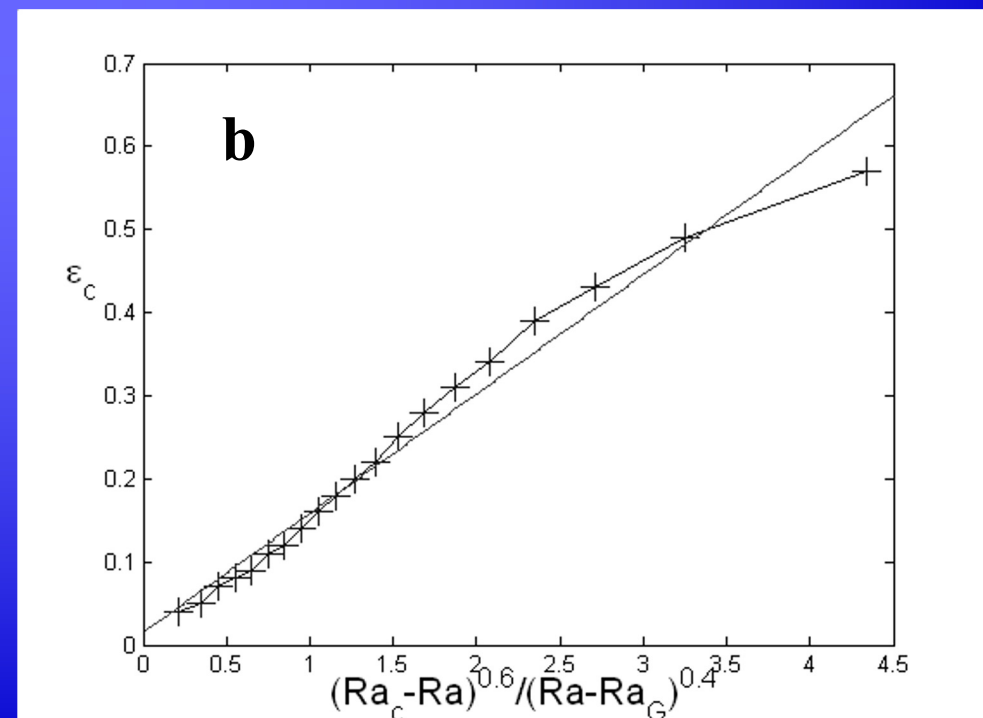
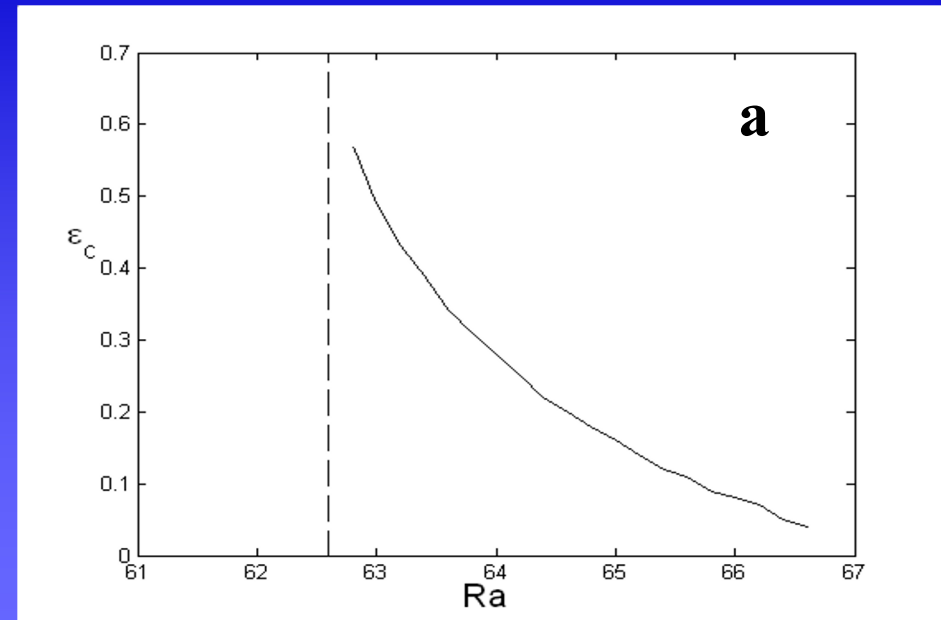
- And

$$\|\exp(A_c t_{\max})\| = \sigma_1 = G_{\max}$$

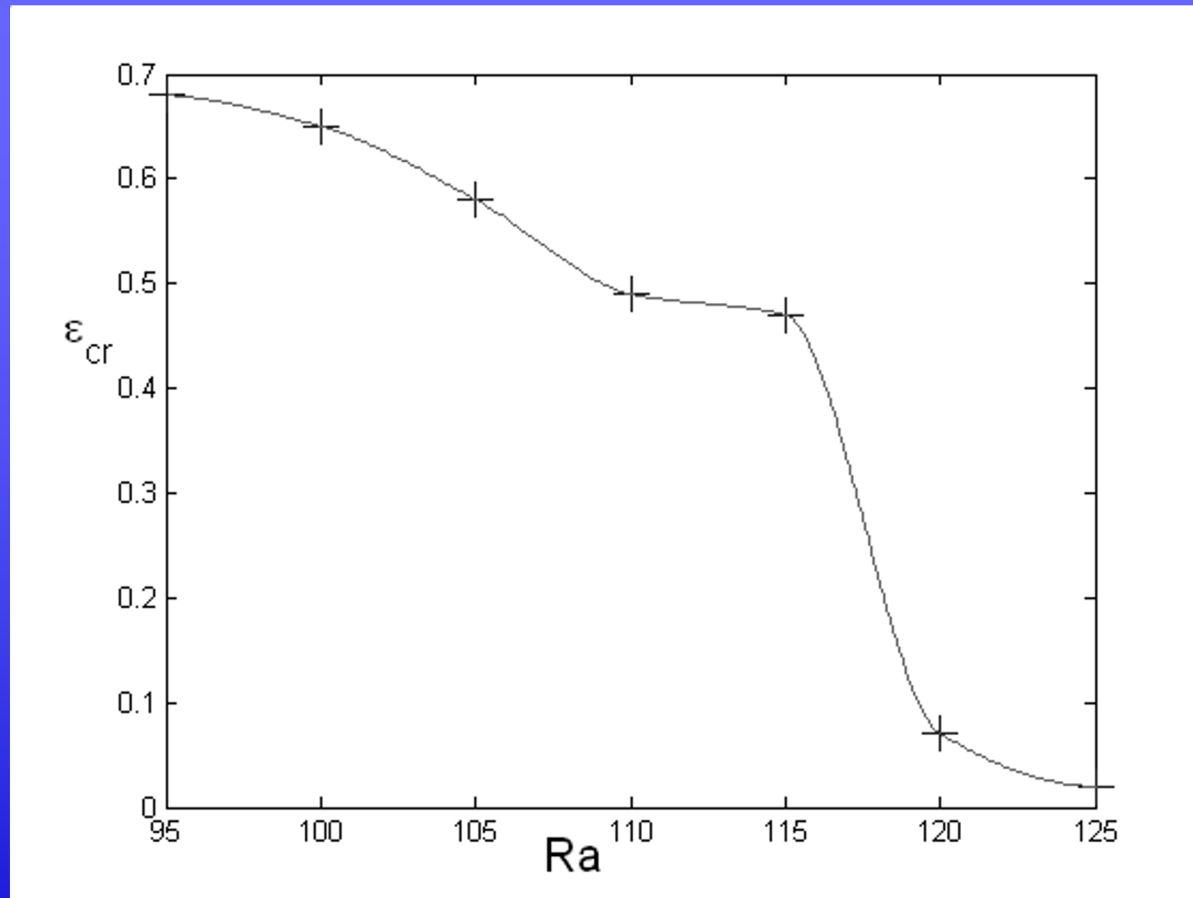
The temperature T at $(x,y)=(1/8, 0)$ is depicted as a function of time. Ad-hoc proportional controller, $Ra=66$, and $Kp=8.4$. The disturbance amplitude is, respectively, 0.07 and 0.08 in (a) and (b).



The critical disturbance amplitude ε_c defining the basin of attraction of the controlled state as a function of the Rayleigh number (a) and as a function of $(Ra_c - Ra)/(Ra - Ra_G)^{0.6}$ (b). Ad hoc proportional controller. $Kp=8.4$.



The critical amplitude of the optimal disturbance depicts as a function of the Ra number for the H₂ optimal controller



Summary of the DLRB problem

- Linear proportional, quadratic Gaussian, and suboptimal H_∞ controllers stabilize the no-motion state of the **RB** problem.
- The ad-hoc, linear, proportional controller is capable of increasing the critical Rayleigh number for the transition from the no-motion state to the motion state by nearly a factor of 2.
- Since the plant is stabilizable and detectable, the synthesized suboptimal and quadratic Gaussian regulators H_2 do not have any limitations in terms of the magnitude of the Rayleigh number.

Limitations of the linear controllers

- Possible saturation of the actuators
- Non-normality of the controlled system
 - The increasing non-normality of the linear operator as the Rayleigh number increases implies that disturbances may amplify a great deal before they eventually decay.
 - Large disturbances render the neglected nonlinear dynamics important.
 - Non-normality also causes numerical difficulties in the calculation of the controller gains.

Outlook

- Linear control theory is a very powerful design tool, but it does not adequately address the adverse effects of nonlinearities
- Methods for developing low dimensional models need to be developed to achieve effective controllers and estimators that can be implemented in practice
- There is a need to develop algorithms to optimize the number and positions of the sensors and actuators

ACKNOWLEDGMENTS

This work was supported, in part, by grant CTS-0212998 from the National Science Foundation

I am indebted to graduate and undergraduate students who contributed to the flow control project, in particular

J. Singer (MS), Y. Wang (PhD), G. Fiedler (MS), J. Tang (PhD), P. Yuen (PhD), and M. Remillieux (BS) and H. Zhao (PhD).